PROCEEDINGS, 50th Workshop on Geothermal Reservoir Engineering
Stanford University, Stanford, California, February 10-12, 2025
SGP-TR-229

Advective Flow in a Conductivity-Dominated Crust: an Example from FORGE

Peter Leary[1] & Peter Malin[2]

[1]Geoflow Imaging Ltd 43 High St, Auckland 1010, New Zealand

[2]Earth and Climate Sciences Duke University

peter@geoflowimaging.com ; malin@duke.edu

Keywords: EGS; crustal heat transport; crustal fluid advection; induced seismicity; Peclet number; ambient crust poro-permeability

ABSTRACT

As recognized in the 1970s, extracting heat from the crust is limited by slow thermal conduction rates. Heat mining was thus predicated on engineering large volumes of permeable rock within hot ambient crust – primarily by hydraulic fracture stimulation. However, engineering such volumes has proved elusive, with many unforeseen outcomes. We describe how such behaviour can arise in crustal rock, illustrating our discussion using circulation test and microearthquake data from the FORGE site.

In the recent post-stimulation circulation test at FORGE, of the many stages treaded the flow at one location was singularly larger than the others. This outcome, along with the spatial distribution of the seismicity induced by the fracture stimulation, is indicative of a critical state permeability system. Its existence in the crust at FORGE - and at many other EGS sites - is supported by a very common permeability characteristic of well logs and cores. It is also consistent with the flow history observed at the singular site, which we model here.

In critical state systems, properties such as permeability can follow statistical distributions that do not cluster around a central average size (as in a bell curve) and are not spread out evenly or equally in space (as in a random medium). Instead, the distribution of FORGE flow data - and prevailing log-and-core permeability observations – show that a small number of permeability channels can greatly exceed a score of others (as in a lognormal curve) and can be localize and unequally spread out (as in a power law medium). The FORGE iMeq data follows this same spread of size and spacing.

The singularly large flow at FORGE was a steady 30 day, 30L/s of stream of 185°C water transiting across the 100 m separated doublet. We suggest that if this location were a simple, isolated fracture between the wells, it would likely have experienced noticeable cooling – dropping the equivalent to less than 100°C in 100 days. Instead, it seems that the steady singular flow is the result of the stimulation connecting to a large size and infrequent spacing natural permeability channel. We model this possibility here and show how this point of view can guide further EGS developments.

1. INTRODUCTION

Wellbore production of geothermal energy has long been seen in terms of crustal heat transfer by thermal conduction and advection. Thermal conduction offers an inexhaustible heat supply at drillable depths in ambient continental crust. Thermal advection offers heat transfer in limited zones of connected fractures. This duality was recognized in a 1980 energy review :

> [M]ost of the potentially exploitable geothermal heat is stored in dry rock……[I]t will be necessary not only to supply the working fluid by injecting water, but also to find or create in some way a permeable network of channels through which the water can flow to be heated. *Energy in Transition, 1985-2010: Final Report The National Academies Press. https://doi.org/10.17226/11771*.

Five decades on, the promise of unlimited clean baseload electrical power from crustal heat conduction and found or created advection is now being pushed forward at sites like FORGE Utah and Blue Mountain Nevada*. What has been going on in the meanwhile – and what might be going on at these and other efforts? In this paper we address a potential source causing this long ramble and how it continues to reappear, for example, at FORGE.

* https://science.utah.edu/faculty/faculty-research/breakthrough-forge/
* https://www.thinkgeoenergy.com/fervo-energy-reports-breakthrough-in-field-scale-egs-project-in-nevada/

2. SOME BACKGROUND AND AN ANSWER IN A (HARD) NUTSHELL

A 2014 survey cites 57 active advection geothermal sites and 3 active conduction sites [1 Moeck & Beardsmore 2014]. A 2020 survey of geothermal projects requiring crustal flow simulation -- termed Engineered Geothermal Systems = EGS -- identifies 24 projects as achieving at least in some success, but only a small number of these can be denominated as conductive rather than advective [2] Pollack, Horne R & Mukerji WGC2020]. By these measures, EGS conductivity-based projects fall systematically short.

Why?

Following oil/gas practice, crustal fluid flow properties have been taken to conform to a statistical ideal in which porosity and permeability variations are assumed to be uncorrelated (random) above a limited length scale. In this model, the crust is effectively a uniform elastic continuum in which engineered fractures are oriented along the local stress field. Above this scale porosity and permeability would be statistically unrelated and uniformly distributed – which is known in critical state systems as uncorrelated white noise. Instead, well-log, well-core, and well-flow data show that porosity and permeability are related and spatially correlated at all length scales: permeability k(x,y,z) is related to porosity φ(x,y,z) by $k=k_o\exp(\alpha\varphi)$.

If φ's population and spatial distributions are bell curve and critical state systems pink noise instead of white (i.e. φ (s) = 1/s, s = spatial frequency), then κ's population and spatial distributions are lognormal and pink.

The result is the presence of singular flow channels at every reservoir scale. The solution to successful EGS would then be to locate and focus on developing these irregular channels. The former could be done using mapping methods such as passive seismic emission tomography to locate natural large-flow channels[#]. The latter by selecting only these crustal flow zones for stimulation.

While φ centers around an average, lognormally distributed k has a few large values whose locations dominate the permeability field. This poro-perm relationship is found in all types of brittle rock. Permeability stimulation induced microearthquakes (iMeqs), including those at FORGE, follow these relationships. FORGE iMeq s are pairwise statistically correlated as G(r) ~ 1/r, r = the distance between iMeq-pairs. This matches κ's distributions for the case of a normal population and pink distributed φ and implies the iMeqs are mapping the permeability structures as well. Since k is lognormally distributed, there will be a few locations with highly elevated permeability. One such permeability structure is reported for the FORGE site stimulation.

What follows here is an accounting of the stimulation flow results reported recently by FORGE in the context of critical state, lognormal and pink noise crustal permeability. A central part of this discussion relates to how such a system can account for the continued energy flow from the singular channel.

3. ELEMENTS OF ADVECTION HEAT TRANSPORT FOR FORGE EGS FLOW STRUCTURE

The Utah Forge second pass stimulation conducted in April-May 2024 sought sustained flow across the 100m well-pair interval diagrammed in Fig 1. The reported well-to-well break-through flow was achieved at a single site along the dotted wellbore trajectory. Fig 2 shows views of the microseismicity generated by the EGS stimulation; shaded rectangles indicate the flow stimulation wellbore interval. Fig 3 displays the initial 9-hr stimulation breakthrough flow data.

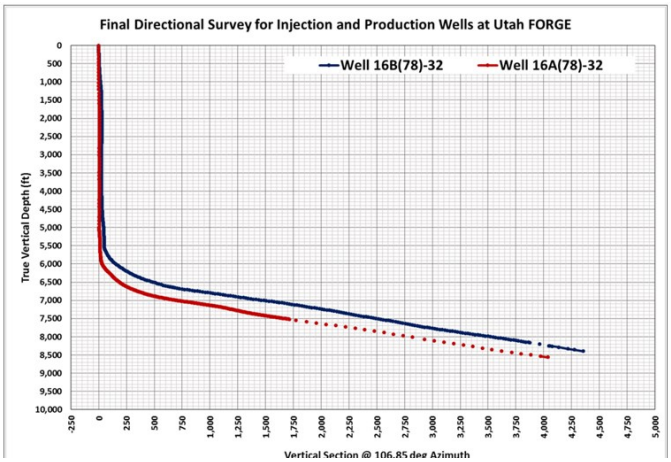

Figure 1. FORGE EGS project well-pair trajectory. Energy and Geoscience Institute at the University of Utah. (2024). Utah FORGE: Wells 16A(78)-32 and 16B(78)-32 Stimulation Program Report - May 2024 [data set]. Retrieved from https://gdr.openei.org/submissions/1695.

https://ambientreservoir.com/services-papers

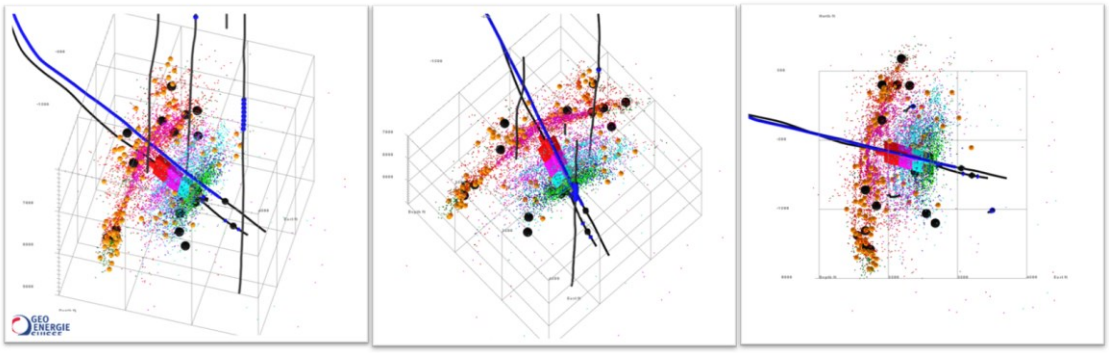

Figure 2. FORGE EGS project well-pair stimulation iMeq activity. Energy and Geoscience Institute at the University of Utah. (2024). Utah FORGE: Wells 16A(78)-32 and 16B(78)-32 Stimulation Program Report - May 2024 [data set]. Retrieved from https://gdr.openei.org/submissions/1695 .

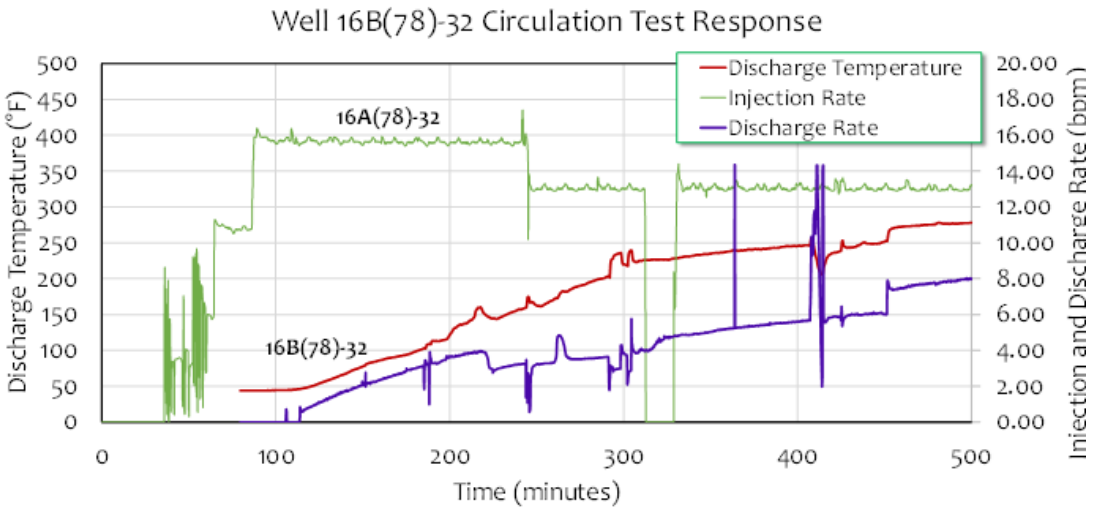

Figigure 3. FORGE EGS project well-pair stimulation break-through well-flow pressure and temperature data. Energy and Geoscience Institute at the University of Utah. (2024). Utah FORGE: Wells 16A(78)-32 and 16B(78)-32 Stimulation Program Report - May 2024 [data set]. Retrieved from https://gdr.openei.org/submissions/1695 .

Judging from the Fig2 iMeq distribution, the well-to-well stimulation flow plane is more or less vertical and more or less oriented along the visible iMeq azimuthal trend. EGS stimulation iMeqs from the first stimulation pass conducted in April 2022 documented the lognormal size distribution and the spatial correlation function of iMeq -pair offset r as $G(r) \sim 1/r$ for $20 < r < 400$ [8 Leary & Malin 2023]. The 2024 iMeqs logically have the same size and spatial correlation distributions and thus accord with the ambient crust poro-permeability empiric $\kappa(x,y,z) \sim \exp(\alpha\varphi(x,y,z)$ as discussed in [8]. On Fig 2 iMeq evidence, EGS fluids injected prior to well-to-well break-through flow follow poro-perm connectivity pathways within the ambient crust and thus do not create stress-oriented planar cubic-law flow structures as envisioned by standard EGS scenarios [6]. In line with the large-scale iMeq trends in Fig 2 we can logically suppose that the well-to-well break-through flow occurs along a 100m reach of stimulation flow connectivity that trends both vertically and horizontally.

In accordance with the expression relating observed wellbore stimulation flow V to Darcy flow v_0 at wellbores, $V \sim \pi/2 r_0 \varphi v_0 \ell$, we picture a hypothetical stimulation flow system geometry as in Fig 4: a bounding crustal volume 100m on a side transfected by a

notionally 20m thick stimulation section of effective porosity $\varphi \sim 0.1$. In this stimulation scenario, well-to-well flow in the hypothetical section begins and ends with Darcy $v_0 \sim 0.1$m/s inflow/outflow at wellbore radii $r_0 \sim 0.1$m. We further suppose that well-to-well fluid flow v(r) away from the wellbores is given by conservation of mass $rv(r) = r_0v_0$. Applying the standard EGS stimulation scenario, we can thus picture an estimated Darcy velocity in the 2b-wide stimulation section as $v_L \sim r_0v_0/L \sim .01/50 \sim 2\ 10^{-4}$m/s. By standard EGS scenarios, this Darcy flow passively absorbs heat from the enclosing crustal volumes [6 Setter et al 2011].

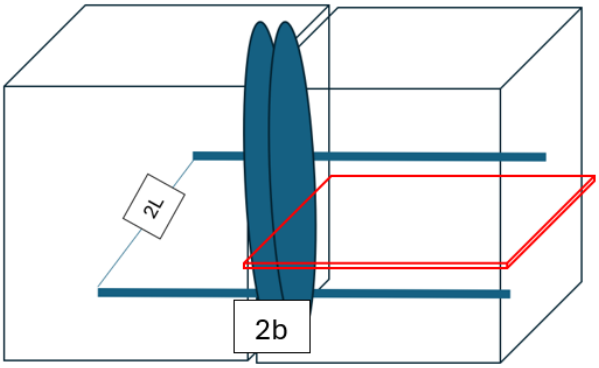

Figure 4. Schema of FORGE well-to-well stimulation flow geometry. A crustal block drilled through by parallel wellbores 2L ~ 100n apart (blue liners) is transected by a stimulated permeability layer of width 2b (blue disks). In the standard EGS heat extraction scenario for pure conduction heat exchange, fluid passing from the inflow wellbore through the stimulated permeability layer to the outflow wellbore absorbs heat from the transection walls. The rate of conductive heat extraction is $Q(y,t) \sim 1/(\sqrt{(t)}\exp(-(\beta y)^2/4Dt)$, t = time, y = distance along the transect, D = crustal thermal diffusivity, and $\beta = D/Ub$ is the inverse Peclet number given fluid flow velocity U and transect half-width b [6]. As distinct from pure conductive EGS heat exchange, the red layer abutting the stimulation zone represents section of poro-permeable crust $\kappa(x,y,z) \sim \exp(\alpha\varphi(x,y,z)$ supporting advective fluid flow into the stimulation layer as per Fig 6.

4. THE SINGULAR FLOW'S HEAT DELIVERY AND IT'S CONSEQUENT PECLET NUMBER.

We look at the recent Utah Forge EGS project system in which well-to-well stimulation flow over a 100m interwell interval recorded a wellbore volumetric flow V ~ 30L/s for 30 days at a steady T = 185°C [3 FORGE2024]. We consider what this flow would imply in terms of a purely conduction source for the heat entering the production well. In arriving at this measure, it is important to keep in mind that in a standard Darcy flow model the rate of heat transfer from the rock depends on the flow speed times the flow-length vL in units of m^2/s relative to the rock-water thermal diffusivity $D \sim 10^{-6}$ m^2/s. The controlling factor is termed the Peclet number Pe = vL/D. We can use the Peclet number to gauge the overall flow system Peclet number and compare this with EGS models for heat transfer by thermal conduction.

The wellbore flow heat production is $Q = \rho CVT \sim 23$MWW ($\rho C \sim 1000$kg/m x 4200 J/kg/°C, $V \sim 30 \times 10^{-3}$ m^3/s, T ~ 185°C). From the observed wellbore flow V the crustal fluid Darcy velocity $v_0 \sim 0.1$m/s follows from $V \sim \pi/2r_0\varphi v_0\ell$ for $\ell \sim 20$m the wellbore axial length open to crustal fluid inflow, $r_0 \sim 0.1$m the wellbore radius, $\varphi \sim .1$ the mean crustal porosity, and $\pi/2$ the quarter-circle perimeter of the combined well-to-well fluid flow leaving/entering the wellbores. The Darcy flow velocity $v_0 \sim 0.1$m/s over an $\ell \sim 20$m open hole interval translates into a Peclet number per unit wellbore length

$$Pe \sim \pi/2r_0\varphi v_0/20/D \sim 75,$$

for $D \sim 10^{-6}$ m^2/s is rock-water thermal diffusivity K/ρC for rock thermal conductivity K ~ 3W/m/°C.

4.1 The Role of Heat Transfer from Rock by Advection

EGS well-to-well Pe ~ 75 flow challenges the exclusive role of thermal conductivity in accessing crustal heat. Somehow, it appears, pure conduction fuels a wellbore fluid flow that carries 75 times more heat than conduction alone supplies. Accordingly, we may reprise the 1980 geothermal energy appraisal in modern terms. Instead of a heat conduction-only medium, the ambient crust is a poro-permeable medium given by the empiric $\kappa(x,y,z) \sim \exp(\alpha\varphi(x,y,z)$, with porosity ($\varphi(x,y,z)$ a spatially correlated pink noise distribution across five decades of scale length (cm-km), and the resultant permeability is lognormal across all scales [4 Leary et al 2019; 5 Malin et al 2020]. It follows that where once heat transfer in the tectonically passive crust was described by conduction alone [6 Sutter 2011],

$$\partial T/\partial t = D\, \partial^2 T/\partial x^2, \quad (1)$$

allowance should be made for heat transport by fluid moving at velocity v past the source rock as per the advection-conduction equation [7 Socolofsky & Jirka 2005],

$$\partial T/\partial t + v\partial T/\partial x = D\, \partial^2 T/\partial x^2. \quad (2)$$

Prompted by the Urah Forge EGS Pe ~ 75 wellbore outflow from a 2L ~ 100m-scale crustal stimulation domain, we here assess how advection velocity $v_L \sim 10^{-6}$m/s can arise to be consistent with the Peclet condition $Pe = v_L\, L/D \sim 75$.

5. THE CONSEQUENCES OF ASSUMING THE HEAT PRODUCTION PURELY BY DIFFUSIVITY D.

Fig 5 assesses how well the standard EGS conduction heat drainage scenario works in flowing fluid at velocity $v_L \sim 2\ 10^{-4}$ m/s over the 30-day heat exchange recorded for the FORGE singular flow. Each Fig 5 panel shows the rate at which heat is extracted over time in days by V_L flow measured at the outflow well at y = 100m given by $Q(y,t) \sim 1/(\sqrt{(t)}\ \exp(-(\beta y)^2/4Dt)$, D = thermal diffusive of rock-fluid system, t = time, y = distance along boundary fracture, and $\beta = D/b\ v_L$ for fluid velocity v_L and fracture half- width b [6]. We note that the term β is the inverse of the model Peclet number.

The upper-left panel in Figure 5 indicates that a 20cm effective width falls short of maximum heat extraction in the allotted time. The lower panels indicate that 1-2m effective stimulation widths rapidly extract too much heat from the crustal block and thus cool the crustal block within the allotted observation time. The intermediate case pictured at the upper-right shows that a slab effective width ~ 60cm is consistent with present observational data at 30 days flow duration. The 60cm effective slab width does not, however, have a long duration at full heat transfer.

Instead, it drains heat from the crustal store at a rate that reduces the transfer by 50% at 100 days.

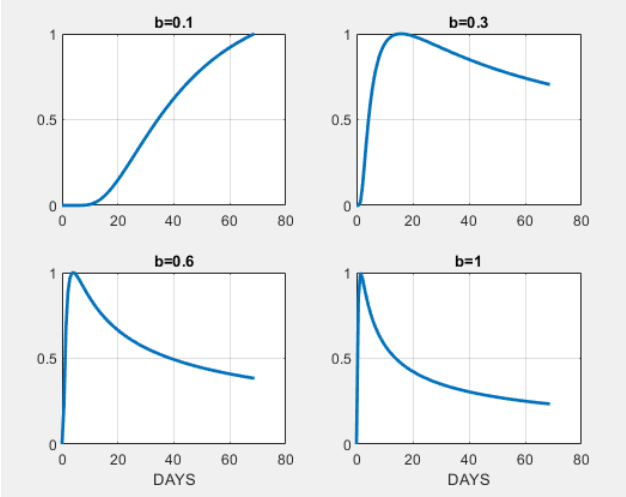

Figure 5. Plots of Q(y=100,t=0:70) heat transport from a purely conductive crust to fracture-borne fluid passing along a boundary surface as pictured in Fig 4. Curves are given by $Q(y,t) \sim 1/(\sqrt{(t)}\exp(-(\beta y)^2/4Dt)$, D = thermal diffusive of rock-fluid system, t = time, y = distance along boundary fracture, and $\beta = D/bv_L$ for fluid velocity v_L and fracture half-width b. Plots show heat flow rate at y = 100m outtake wellbore for a range of fracture gaps given by b = 0.1m to 1m at flow durations measured in days. FORGE well-to-well flow was observed at steady temperature T = 185ºC for 30 days. Pure thermal conduction heat transfer implies that an equivalent fracture half-width b ~ 0.3, with heat extraction decline beginning after 30 days. If the FORGE outflow temperature holds steady for significantly longer than 30 days, it is logical to infer that the FORGE well-to-well fluid heat transfer proceeds by advective fluids as well as by thermal conduction.

If pure conduction is the only heat exchange mode allowed, Fig 5 implies that heat extraction significantly longer than 30 days will start to cool the FORGE system. The more substantive point made by Fig 5 is that pure conductive heat extraction is directly dependent on the physical scale of the heat store. Standard EGS reckons that it is always possible to find a large enough heat store to accommodate a stimulation slab that will permit a commercial heat extraction rate and duration as illustrated by the upper-right panel in Fig 5 , e.g., [9 Jain, Vogt & Clauser2015].

If, however, future observation shows that the FORGE EGS stimulated flow system endures significantly longer than 30 days, the question arises, is the standard EGS pure conduction heat extraction model seen here the complete picture. From Fig 2 iMeq size distribution and spatial correlations, we know that wellbore fluids are not restricted to flow only in the stimulated interval between wells. They can instead pass into the permeable crustal blocks to drain heat stored in hot fluids within a $\kappa(x,y,z) \sim \exp(\alpha\varphi(x,y,z))$ permeability distribution much larger than the 100m-wide stimulation zone.

6. INCLUDING ADVECTED EXTRACTION OF HEAT FROM PINK NOISE DISTRIBUTED POROUS ROCK

Fig 6 expresses the fundamental aspect of advection versus conduction for heat transfer. In solving Eq 2 for the heat transfer associated with the porosity-permeability of a critical state crustal block through which fluid moves at velocity v, we see that advection can outperform conduction in heat transfer. Considering the block to be at an initial unit temperature for distance $0 < x < 1$ into the rock. In Fig 6 fluid moves through the block over a range of velocities, draining the heat at different rates. The black trace profiles the final state temperature after significant advection flow, while red and blue traces profile temperatures for smaller amounts of advection above conduction. The black curves advection velocity drains 10 times more heat than does the red and blue curves conduction.

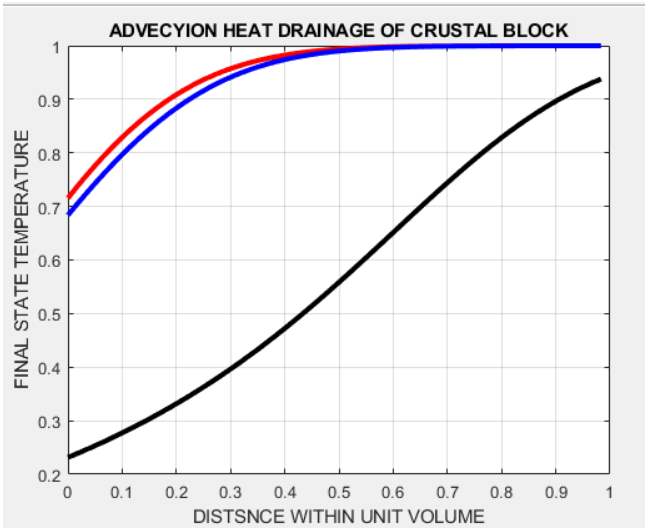

Figure 6. Effect of advection black trace versus conduction (red, blue traces) on draining heat from crustal blocks as represented by the red crustal section in Fig 4. The initial state of the crustal block is unit temperature across a unit volume, and the final state is as shown by the red/blue/black curves. The heat above the conduction profile (red, blue) is only 15% of the heat above the advection profile (black). The time- evolving temperature of a crustal section with fixed temperature at the outer edge and heat flow boundary condition $\partial T/\partial x = hT$, h = heat transfer coefficient, at the stimulation zone on the inner edge. The temperature profiles are solutions to the advection-conduction Eq (2) for advection velocities v that are insignificant (red, blue) and significant (black). While advection clearly drains heat at much faster rates than conduction for any given crustal volume, the functional point is that conductivity is spatially constant at K ~ 3W/m/ºC while permeability and therefore advection domains are spatially highly variable and statistically lognormal.. Fig 2 shows that the FORGE iMeq activity domain and hence the local permeability domain is very much larger than the well-to-well stimulation zone conductivity drainage domain. EGS seismic activity thus signals where and by how much advective heat drainage is accessible to a well-pair. Over a specific time duration, properly located and mapped permeability domains can effectively supply heat from a far larger crustal volume than can conduction alone. We thus look to a long-duration FORGE EGS stimulation flow system as an example of how EGS stimulation can actually work at large in the ambient crust

The Fig 6 temperature profiles are given by Eq (3) from Carslaw & Jaeger (1959, §15.2 *II*):

$$T(x,t) = T_0 - T_0/2\ E1 + - T_0/2\ E2\ ,$$

$$E1 = \mathrm{erfc}((x-vt)/2/\sqrt{Dt}) + Dh/(Dh-v)\ \exp(vx/D)\ \mathrm{erfc}((x+vt)/2/\sqrt{Dt})$$

$$E2 = (2Dh-v)/2/(Dh-v)\ \exp(x-ht(v-Dh))\ \mathrm{erfc}((x+(2Dh-v)t)/2/\sqrt{Dt}), \qquad (3)$$

Where D ~ 1-$^{-6}$ m^2/s is the diffusivity of the rock-water system and h = coefficient of heat transfer at the heat flux boundary condition $\partial T/\partial x = hT$ at x = 0.

The Appendix motivates the functions in Eq (3) and gives a Matlab code for generating Fig 7.

7. APPLICATION OF ADVECTED HEAT TO FORGE WELL-TO-WELL STIMULATION FLOW STRUCTURE

We have seen in Fig 5 that purely conductive heat take-up by fluid moving parallel to the faces of the assumed FORGE EGS stimulation zone in Fig 4 is unlikely to persist significantly beyond the observed 30 days. If the heat take-up is observed to persist, it is likely that advective fluids are bringing heat to the well-to-well flow structure. Accordingly, we consider with Eq (3) how advective fluids can drain heat from the ambient poro-perm crust surrounding the stimulation volume.

As EGS fluid injection increases the stimulation zone permeability, fluids in the abutting low permeability crust under lithostatic pressure will seep into the significantly sub-lithostatic fluids of the stimulation zone. As long as well-to-well flow persists at sub-lithostatic pressures, seepage from the abutting crustal walls will persist. For two walls area A ~ 4000m^2, the seepage volume flow should be some fraction of the well-to-well volume flow V ~ 30L/s ~ 3 10^{-2}m^3/s. Setting $V_s = A\, v_s$, the formation seepage velocity is presumed to be a fraction of 10^{-5} m/s.

We note that Eq (3) is essentially undefined for advection velocities above ~ 10^{-6} m/s for the spatial and temporal dimensions of the FORGE flow system. We can thus expect a formal degree of physical stability for a FORGE EGS advection flow velocity range 10^{-7}m/s < v < 10^{-6}m/s, with the lower limit grading into conduction-only heat transfer. This representative advection velocity range holds for the coefficient of heat transfer h ~ 0.5; smaller values of h narrow the range of advection velocities to lower advection flow values, but do not affect the conduction limit. We find that Eq (3) applied to the FORGE EGS flow leads to a physically plausible set of advection flow and heat transfer parameters.

Fig 7 shows the significant economic benefits of heat transfer for advective over conduction-only heat exchange systems. Each subplot gives final state temperature profiles for crustal heat stores abutting the EGS stimulation zone. Heat is extracted via the heat flux boundary condition $\partial T/\partial x = hT$ at rates given by advective fluid flow velocity v from the crustal heat store into the well-to-well fluid passing through stimulation zone over a period of 1150 days. The three subplot have values of heat transfer coefficient h = 0.5, 0.05, and 0.005 from left to right. The trace colour sequence green, black, gold, red, blue marks the sequence of advective fluid velocities 4.5 10^{-7}, 2 10^{-7}, 1 10$^{-7,}$ 3 10^{-8}, 1 10$^{-8,}$ m/s through the heat store block. The lowest advective velocities equate to pure conductive heat flow into the stimulation zone fluid.

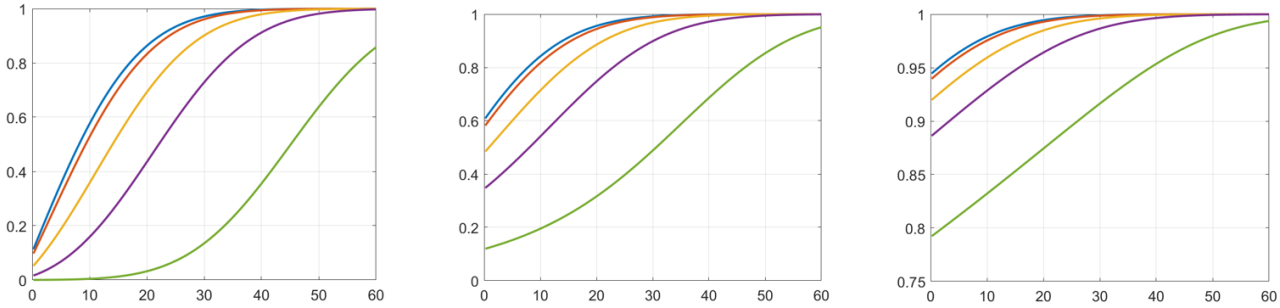

Figure 7. Effect of advection flow on heat extraction for the FORGE EGS well-to-well flow stimulation geometry pictured in Fig 4. Each subplot gives the temperature profiles in the Fig 4 crustal slab in red for a succession of advection velocities v = (0.1 0.3 1 2 4.5) x 10^{-7} m/s denoted by trace colours blue, red, gold, black, green. The profile extend from x = 0 at the flux boundary condition $\partial T/\partial x = hT$ to the fixed temperature boundary condition at x = 60m. From left to right, the three subplots show temperatures for values of coefficient of heat transfer h = 0.5, 0.05, 0.005. The subplot temperature spread decreases with decreasing values of h, but far each value the area above the respective advection velocities curves follow the same pattern, notably the areas above the green curves being five to ten greater than the areas above the blue = conductivity temperature curves. Thus the heat removed by plausible advection processes greatly exceeds the heat removed by conduction. We may logically assign Peclet numbers 0 < Pe < 10 to the displayed advection velocities. Peclet numbers Pe ~ 5-10 have been observed in wellbore-fracture flow data and this can be considered as physically realistic.

The heat transferred from the crustal store to the stimulation zone fluids is a minimum for conduction and maximum for the highest advective flow compatible with the Appendix formulae and Matlab code. The plot area to the left and above the temperature profiles are proportional to the heat extracted by the flux boundary condition. For each subplot, the area above the green traces are respectively 5, 8, and10 times the areas above the conductive limit profiles.

By definition of the Peclet number as ratio of advected to conducted heat, the three plots in Fig 7 are respectively for Pe ~ 5, 8, and 10. We note that deep wellbore temperature data are consistent with fluid flow in fractures delivering heat at for 5 <Pe < 10 [10 Geofluids 2017; 11 Energies 2017]. We further note that the Fig 7 advection fluid flow rates are consistent with flow velocities just above velocities associated with the onset of crustal convection [12 Ingebritsen, Sanford & Neuzil 2008]. Such crustal fluid velocities are consistent both with fluid seepage into the well-to-well stimulation zone interfaces of several thousand square meters, and with the wellbore fluids reaching into the stimulation volume marked out by the Fig 2 iMeq population. The Fig 7 advection-conduction solutions Eq (3) are thus compatible with all presently known features of the FORGE well-to-well flow data.

8. CONCLUSIONS -- EXPLORING/EXPLOITING ADVECTED HEAT EXCHANGE IN K~EXP(α ϕ) CRUST

It follows from the Fig 7 construction that ambient crust fluid advection heat recovery can plausibly be an order of magnitude more effective than pure conduction. Put differently, the Fig 7 constructs have Peclet numbers 5 < Pe < 10, where the conduction-only heat transfer processes are Pe < 1. In the past, the heat conduction constraint was ignored by focussing on access to arbitrarily large heat resources: pump long enough on a large enough crustal volume and all will be well. This scheme fails because it assumes a quasi-uniform poro-elastic continuum in winch fluid is a passive component. External fluids injected into this supposed crustal medium generate stress-aligned planar flow channels from which heat is absorbed conductively as per [6].

Fig 2 FORGE EGS stimulation iMeq data limits this crustal picture. The well-to-well flow phenomenology is encased in a much larger crustal volume of iMeq activity. The Fig 2 iMeq data reprise 2022 stimulation data whose size and spatial correlation distributions are statistically congruent with the near-universal ambient crust poro-permeability empiric $\kappa(x,y,z) \sim \exp(\alpha\varphi(x,y,z))$ [8]. Buried within the Figg 2 iMeq stimulation volume is a well-to-well flow stimulation structure achieved as one of 18 attempts to link the two Fig 1 wells. It is manifest that the achieved EGS well-to-well flow structure is part of a much wider and more erratic stimulation phenomenology than historically supposed. Equally manifest is that crustal fluids play an active rather than passive role in the ambient crust and thus should be adequately accounted for in EGS heat extraction.

FORGE EGS stimulation iMeq data set the context in which effective advective heat transport in occurs. iMeq lognormality and two-point spatial correlations $G(r) \sim 1/r$ are properties of crustal poro-permeability $\kappa(x,y,z) \sim \exp(\alpha\varphi(x,y,z))$. Lognormality guarantees the existence of km-scale high permeability domains allowing fluids to pass at a relatively high flow rates. The pairwise two-point spatial correlation $G(r) \sim 1/r$ validated by FORGE iMeq location statistics indicates a substantial degree of fluid flow connectivity at km scales. These features of the ambient crust account for deep wellbore observation of naturally occurring fracture-borne fluid flow structures of Pe numbers 5 < Pe < 10 consistent with heat transfer inferred from Fig 7 crustal block temperature profiles. We thus see that on scales from 10m to 1km, he empiric $\kappa(x,y,z) \sim \exp(\alpha\varphi(x,y,z))$ provides fertile grounds for EGS exploration and exploitation.

As discussed in [5], EGS is logically applied to crustal volumes identified as emitting seismic energy associated with quasi-active fluid flow structures. The conspicuous intrinsic poro-perm duality with iMeq activity in Fig 2 for the FORGE EGS site is clear evidence that the advective fluid flow incorporated in Fig 7 provides ample seismic emissions by which Seismic Emission Tomography (SET) technology can image the details of fluid flow distribution as per the EGS stimulation structure sketched in in Fig 4 and conceptualised by Eq (3) pictured in Fig 7.

In conclusion, we find that standard conduction-only EGS heat extraction is flawed not only in practice, but in concept. Conceptually, standard EGS ignores the fundamental ambient crust poro-permeability empiric $\kappa(x,y,z) \sim \exp(\alpha\varphi(x,y,z))$ and thus misses three aspects of heat extraction from the ambient crust.

First, lognormality of empiric $\kappa(x,y,z) \sim \exp(\alpha\varphi(x,y,z))$ implies the existence of large-scale permeability domains throughout the ambient crust that potentially can support an EGS development.

Second, the inherent advection nature of a high-permeability domains means that far more heat can be extracted by advection than from comparable crustal volumes through conduction only.

Third, proven Seismic Emission Tomography (SET) technology can locate candidate high-permeability domains in the ambient crust.

All three of these vital EGS factors are present in trial-form at the FORGE project volume and can be explored and exploited in the coming project phases. The present Pe ~ 75 and Q ~ 25MW well-to-well flow facility stands as an observational anchor point by which to scientifically generate an engineering blueprint for commercial ambient crust heat extraction.

REFERENCES

[1] Moeck IS & Beardsmore G (2014) A new 'geothermal play type' catalog: Streamlining exploration decision making, 39th Workshop on Geothermal Reservoir Engineering Stanford University, SGP-TR-202

[2] Pollack A, Horne R & Mukerji T (2020) What Are the Challenges in Developing Enhanced Geothermal Systems (EGS)? Observations from 64 EGS Sites, Proceedings World Geothermal Congress 2020, Reykjavik, Iceland, April 26 – May 2, 2020

[3] Utah FORGE: Wells 16A(78)-32 and 16B(78)-32 Stimulation Program Report - May 2024 -- EOJ Report-may 22 2024-final -- *https://gdr.openei.org/submissions/1695*

[4] Leary P. Malin P, Saarno T, Heikkinen P & Diningrat W (2019) Coupling Crustal Seismicity to Crustal Permeability – Power-Law Spatial Correlation for EGS-Induced and Hydrothermal Seismicity, 44th Workshop on Geothermal Reservoir Engineering Stanford University, 2019 SGP-TR-214 1

[5] Malin PE , Leary PC, Cathles LM & Barton C (2020) Observational and Critical State Physics Descriptions of Long-Range Flow Structures, Geosciences 2020, 10, 50; doi:10.3390/geosciences10020050

[6] Sutter D, Fox DB, Anderson BJ, Koch DL, von Rohr PR, & Tester JW (2011) Sustainable heat farming of geothermal systems: a case study of heat extraction and thermal recovery in a model EGS fractured reservoir, 36th Workshop on Geothermal Reservoir Engineering Stanford University, 2011 SGP-TR-191

[7] Socolofsky SA & Jirka GH (2005) Special Topics in Mixing and Transport Processes in the Environment, Coastal and Ocean Engineering Division. Texas A&M University

[8] Leary P & Malin P (2023) Permeability-Related Spatial Correlation Systematics for FORGE EGS Stimulation iMeqs, 48th Workshop on Geothermal Reservoir Engineering Stanford University, SGP-TR-224 1

[9] Jain C ,Vogt C & Clauser C (2015) Maximum potential for geothermal power in Germany based on engineered geothermal Systems, *Geothermal Energy* (2015) DOI 10.1186/s40517-015-0033-5

[10] Leary P, Malin P & Niemi R (2017) Fluid Flow & Heat Transport Computation for Power-law Scaling Poroperm Media, *Geofluids* **2017**

[11] Leary P, Malin P, Saarno T & Kukkonen I (2017) Prospects for Assessing Enhanced Geothermal System (EGS) Basement Rock Flow Stimulation by Wellbore Temperature Data, Energies 2017, 10, 1979; doi:10.3390/en10121979

[12] Ingebritsen SE, Sanford WE & Neuzil CE (2008) Groundwater in Geologic Processes, DOI:10.1007/s10040-008-0317-y

[13] Carslaw HS & Jaeger J (1959) Conduction of Heat in Solids, Oxford University Press

APPENDIX – MOTIVATION AND MATLAB CODE FOR CARSLAW & JAEGER (1959) §15.2 II. EQ (10)

The combination of Fourier's law of heat flow $Q = K\,\partial T/\partial x$ and conservation of heat energy $T/\partial t = \partial Q/\partial x$, for K~ 3W/m/^{o}C the coefficient of rock heat conduction and $\rho C \sim 4MJ/m^3/^oC$ the volumetric heat capacity of water gives the heat diffusion equation for the rock-water system $\partial T/\partial t = D\,\partial^2 T/\partial x^2$ for system thermal diffusivity $D \sim 10^{-6}$ m^2/s . The core solution to the 1D diffusion equation is $T(x,t) \sim \exp(-x^2/4Dt)/\sqrt{(4\pi Dt)}$. Solutions to the diffusion equation involving boundary condition often require evaluating the spatial integral of $\exp(-x^2/4Dt)/\sqrt{(4\pi Dt}$, leading to terms in the error function given by $\mathrm{erf}(x) = 2/\sqrt{\pi}\int_0^x \exp(-z^2)dz$ and/or its complement $\mathrm{erfc}(x) = 1 - \mathrm{erf}(x)$. Accordingly

The advection-diffusion equation $\partial T/\partial t + v\partial T/\partial x = D\,\partial^2 T/\partial x^2$ arises from what is in effect the diffusion equation in a reference system moving at velocity v relative to the diffusion system. Accordingly, solutions to the advection-diffusion equation can take forms such as
$T(x,t) \sim \mathrm{erf}((x+vt/2)/\sqrt{(4Dt)}) - \mathrm{erf}((x-vt/2)/\sqrt{(4Dt)})$ that describe temperature distributions due to point source heat injected into a porous medium with moving fluids.

As per these notes. the Carslaw & Jaeger §15.2 II. Eq (10) solution for heat transported across a porous crustal block by fluids moving at velocity U with fixed temperature boundary at one end and a heat flux condition $\partial T/\partial x = hT$ at the opposite end is expressed in terms exponential and complimentary error functions. The Fig 7 plots are computed by the below Matlab code evaluations of exp and erfc functions.

```
clear
```

```
x=0.01:.01:3;x=x*20;D=1e-6;T0=1;t0=1e3;t1=10000e4;
nt=100;t__=logspace(log10(t0),log10(t1),nt);
nv=5;v_=[.1 .3 1 2 4.5]*1e-7;
nh=3;h_=[.5 .05 .005];
for ih=1:3   h=h_(ih);
    for iv=1:5   v=v_(iv);U=v;
%
for it=1:nt t=t__(it);
E1=erfc((x-U*t)/2/sqrt(D*t)) + D*h/(D*h-U)*exp(U*x/D).*erfc((x+U*t)/2/sqrt(D*t));
E2=(2*D*h-U)/(D*h-U)*exp(h*x - h*t*(U-D*h)).*erfc(  (x + (2*D*h-U)*t)/2/sqrt(D*t)  );
T=T0*(1-E1/2+E2/2);
T_(:,iv,ih)=T;A(iv,ih)=300-sum(T);
end
end;end
%
```